RESEARCH MEMORANDUM

A LOW-PRESSURE-LOSS SHORT AFTERBURNER FOR SEA-LEVEL THRUST AUGMENTATION

By Carl C. Ciepluch, Wallace W. Velie, and Richard R. Burley

Lewis Flight Propulsion Laboratory
Cleveland, Ohio

DECLASSIFIED
ATS 480

AUTHORITY
DROBKA TO LEBOW
MEMO DATED 12/13/65

NATIONAL ADVISORY COMMITTEE
FOR AERONAUTICS

WASHINGTON

June 7, 1955

NACA RM E55D26

NATIONAL ADVISORY COMMITTEE FOR AERONAUTICS

RESEARCH MEMORANDUM

A LOW-PRESSURE-LOSS SHORT AFTERBURNER FOR SEA-LEVEL THRUST AUGMENTATION

By Carl C. Ciepluch, Wallace W. Velie, and Richard R. Burley

SUMMARY

An investigation of the problems associated with the design of a low-pressure-loss, short afterburner for sea-level thrust augmentation was conducted in a static, sea-level test stand using the power section of a 5970-pound-thrust, axial-flow turbojet engine.

A $11\frac{1}{2}^{o}$ innerbody diffuser with turbine-discharge flow-straightening vanes installed had the lowest pressure loss of any of the diffusers investigated. The tail-pipe pressure loss was reduced 1 percentage point by fairing (flattening) the afterburner fuel-spray bars, which were located in the high Mach number, turbine-discharge flow.

The total-pressure loss of a 28-spray-bar, short-afterburner configuration was 5.5 percent of the turbine-discharge pressure, which was approximately equal to the loss of the standard engine tail pipe. Because the tail-pipe pressure loss of the short afterburner was about equal to that of the standard engine tail pipe, the nonafterburning specific fuel consumption of the engine equipped with a short afterburner would be equal to that of the standard nonafterburning engine.

The 28-spray-bar, short-afterburner configuration had a peak combustion efficiency of 0.95 at an over-all fuel-air ratio of 0.045. Maximum thrust augmentation of 1.44 was obtained with this short afterburner.

INTRODUCTION

Long-range turbojet bomber and transport aircraft may require some means of thrust boost or augmentation for take-off. The typical afterburner augmenter usually adds to the nonafterburning-engine pressure losses and thereby reduces aircraft cruising range. A program is therefore being conducted at the NACA Lewis laboratory to investigate the problems associated with the design of low-pressure-loss, light-weight afterburners for this application. The length of the afterburner was arbitrarily

limited to that of the standard engine tail pipe (approximately $4\frac{1}{2}$ ft). As a result of the limited length available for the afterburner, both the afterburner-diffuser and combustion-chamber lengths had to be considerably shorter than those usually used in afterburners.

Initial phases of the program are reported in references 1 and 2, which present the performance of several short annular diffusers and the afterburning performance of several short afterburners, respectively. Although a maximum thrust augmentation of 1.33 was obtained with one short-afterburner configuration described in reference 2, the specific fuel consumption during nonafterburning (cruise condition) was 3 percent higher than that of the standard engine because of the increased pressure loss of the short-afterburner tail pipe.

The purpose of the investigation reported herein was to extend the diffuser work of reference 1 in an attempt to decrease afterburner pressure losses and to improve upon the thrust augmentation obtained by the short afterburners in reference 2.

Afterburner pressure loss and over-all performance were obtained in a static, sea-level test stand with the engine operating near rated conditions. The nonafterburning total-pressure losses of both diffuser configurations and afterburner components were obtained. Afterburning performance data were obtained over a range of fuel-air ratios at approximately rated engine conditions.

APPARATUS

Engine and Installation

The engine used for the investigation was a production-model turbojet engine with a 5-minute military thrust rating of 5970 pounds at 7950 rpm and an exhaust-gas temperature of 1275° F at static, sea-level conditions. A cross-sectional view of the engine with a typical short-afterburner tail pipe installed is shown in figure 1.

The engine was mounted in a static, sea-level test stand as illustrated by the schematic diagram in figure 2. Engine thrust was transmitted to and measured with a null-type, balanced-air-pressure diaphragm. A diaphragm-type seal was used to isolate the sound-muffling exhaust chamber from the test cell. Engine-inlet air temperature was controlled with a can-type combustion preheater. The engine air flow was measured by a calibrated air-measuring nozzle in the atmospheric-air inlet line and by a flat-plate orifice in the preheater line.

Short-Afterburner Components

The afterburner components used during this investigation are shown in figures 3 to 5.

Afterburner shell. - A single afterburner outer-shell contour was used throughout the investigation and is shown in figure 3(a). An 8-inch, constant-area, annular section was added to the tail pipe downstream of the turbine to accommodate the instrumentation that was used to measure turbine-discharge total pressure ahead of the diffuser inlet. A 4-inch spool section was added just ahead of the exhaust nozzle to facilitate measuring exhaust-nozzle-inlet total pressure. The over-all length of the afterburner (from the diffuser inlet to the end of the exhaust nozzle) was 57.6 inches. This length does not include the 8-inch constant-area section downstream of the turbine. Also included in figure 3 for comparison is an 18-inch conical innerbody diffuser and tail-pipe assembly that was used during the investigation of reference 1 and the standard engine tail pipe.

Innerbodies. - The three conical innerbodies shown in figure 4(a) were used during the investigation. The $11\frac{1}{2}^{\circ}$ and 15° innerbodies were approximately 18 inches in length, and the 20° innerbody was approximately 12 inches in length.

Turbine-discharge flow-straightening vanes. - Two types of turbine-discharge flow-straightening vanes were investigated; the physical details of each are shown in figure 4(b). One type, referred to as the sheet-metal straightening vanes, was similar to that designed in reference 1. These straightening vanes were simple, sheet-metal, constant-curvature vanes originally constructed in two parts (to correct varying amounts of whirl across the passage). However, the part of the vane that was mounted on the outer shell (ref. 1) was not used during this investigation; only the part that was mounted from the innerbody was used. There were 37 vanes equally spaced around the circumference of the diffuser inlet at the location shown in figure 3(a).

The other type of vane, referred to as the cast straightening vane, was designed by the engine manufacturer for an afterburning model of the engine used during this investigation. These vanes were cast in one piece and were twisted to correct for the varying amount of turbine-discharge whirl. The vanes had a 2-inch cord. They were mounted, equally spaced, on the outer shell at the diffuser inlet and did not extend to the innerbody (fig. 3(a)). A total of 59 of these vanes was used.

Fuel-injection systems. - Afterburner performance data were obtained with two different fuel-injection systems. One system consisted of 28 round spray bars equally spaced around the circumference of the afterburner with five orifices per bar injecting fuel upstream. The other system consisted of 16 faired spray bars equally spaced around the circumference of the afterburner with ten orifices per bar (five orifices per side, diametrically opposite each other) injecting fuel normal to the flow. A comparison of the profiles at the round and faired spray bars is shown in figure 5(b). The faired spray bars were faired gradually in order to prevent restricting the fuel flow to the last orifices. The spray-bar fuel orifices were located radially in the following manner: The annular flow passage at the fuel-injection plane was divided into six equal annular areas, and the orifices were positioned in the spray bars at a point coinciding with the center of each of the annular-area increments except the one nearest the afterburner shell. The fuel-injection spray bars were located just behind the straightening vanes, approximately 5.25 inches downstream of the diffuser inlet. Spray-bar fuel orifices were 0.041 inch in diameter.

3679

Flameholder. - The flameholder used during this investigation is shown in figure 5(c). The flameholder, which consisted of two V-gutter rings 0.75 inch in width, was mounted 1 inch downstream of the diffuser innerbody. Flameholder blockage is approximately 14 percent.

Liner. - The afterburner outer shell was equipped with a perforated liner (fig. 5(a)) similar to the one used in reference 2. The liner was made of 1/16-inch Inconel sheet, and there was a 0.3-inch opening between the liner and the outer shell at the upstream end of the liner to capture turbine-discharge air for cooling of the outer shell. Liner perforations were 3/16-inch-diameter holes spaced so that the centers were 1/2 inch apart.

Exhaust nozzles. - During nonafterburning operation (tail-pipe pressure-loss investigations), a 20.5-inch-diameter nozzle with a tab adjustment was used to obtain the desired engine operating conditions. Conical exhaust nozzles with exit diameters of 24.25, 25.5, and 26.0 inches were used to obtain afterburning performance.

INSTRUMENTATION

Exhaust-nozzle-exit static pressure was measured by static taps located in the sound-muffling exhaust chamber. The engine-inlet pressure was assumed to be equal to the test-cell static pressure. The turbine-discharge total pressure was measured near the end of the 8-inch constant-area annular section ahead of the diffuser inlet.

The location and amount of instrumentation used during the investigation are shown in figure 1. Diffuser-outlet (station 7) whirl and static-pressure profiles were measured with a radially movable, wedge-type probe,

which consisted of a 7° wedge with a static-pressure tap on each face. In order to measure the diffuser-outlet whirl angle, the probe was positioned radially in the flow passage and was rotated on its axis until the pressure on each face of the wedge was equal; the whirl angle was then determined from the position of the probe and a previous calibration. The stream static pressure was obtained by averaging the values from the wedge-face static-pressure taps.

The total-pressure probes used to measure total pressure at the turbine discharge, diffuser outlet, and exhaust-nozzle inlet had a 30° internal chamber. These probes were able to recover approximately 100 percent of the velocity head up to an angle of attack of approximately 20°. Above a whirl angle of 20° the total-pressure measurements were corrected to true stream values.

Primary-engine-combustor fuel flow was measured with a calibrated rotameter, and afterburner fuel flow was measured with a vane-type electronic flowmeter.

PROCEDURE

All short-afterburner performance data were obtained at an engine speed of 7900 rpm, a turbine-discharge temperature of 1240° F, and an engine-inlet temperature of 100° F. These engine operating conditions were slightly less than the 5-minute military ratings and were used to ensure longer engine life.

The pressure loss of the standard, nonafterburning-engine tail pipe was determined in order to provide a basis for comparison with the pressure loss of the final afterburning configurations. During the diffuser investigation the fuel-spray bars, flameholder, and liner were not installed. The pressure losses of these components were measured individually while installed in the diffuser configuration with the best over-all performance.

Afterburning performance was obtained with three fixed-area conical nozzles which resulted in three over-all engine fuel-air ratios at the specified engine operating conditions. The afterburner was lighted by hot-streak ignition originating in one of the primary combustors.

RESULTS AND DISCUSSIONS

Diffuser Pressure Losses

Effect of turbine-discharge flow-straightening vanes on diffuser performance. - Whirling flow often exists at the turbine discharge of turbojet engines. The effect of various amounts of whirl on the performance of annular diffusers with constant-diameter outer shells and

[redacted]

converging innerbodies is reported in references 3 to 5. In reference 1 (short-afterburner diffuser tests) whirling flow up to an angle of 20° was encountered at the turbine discharge. Reduction of this whirl with the use of turbine-discharge flow-straightening vanes resulted in a marked decrease in over-all diffuser pressure loss. Consequently, the first step in the reduction of afterburner pressure loss was the elimination of turbine-discharge whirl.

The effect of the cast straightening vanes on diffuser-outlet whirl and velocity profiles is shown in figure 6. Whirl was most severe near the innerbody (fig. 6(a)) with a whirl angle of approximately 40° existing at the innerbody wall. The large whirl angle near the innerbody was a result of the amplification of turbine-discharge whirl necessary to maintain constant, streamline, angular momentum. By installing the cast straightening vanes at the turbine discharge, the diffuser-outlet over-all whirl was effectively reduced, although a region of high whirl remained near the innerbody. This region of high whirl near the innerbody was caused by the fact that the cast straightening vanes did not extend to the innerbody (fig. 6(a)). The reduction in over-all whirl with the use of the straightening vanes resulted in a decrease in tail-pipe pressure loss (ratio of loss in total pressure between turbine discharge and exhaust-nozzle inlet to turbine-discharge total pressure) from 0.056 to 0.034.

3678

The velocity profiles (fig. 6(b)) were determined from the ratio of local static to total pressure by using one-dimensional flow relations. Total-pressure measurements, which were obtained with a fixed rake, were corrected to true stream values when necessary, and, therefore, the calculated velocities presented are true stream values. The velocity profile of the diffuser with the cast straightening vanes was relatively uniform compared with the profile of a diffuser without straightening vanes.

A comparison of diffuser-outlet whirl and velocity profiles for both types of straightening vanes with the $11\frac{1}{2}^{\circ}$ diffuser is shown in figure 7. Except in the region of the innerbody, the cast straightening vanes appeared more effective in reducing over-all whirl. They also provided a more uniform velocity distribution at the diffuser outlet. The tail-pipe pressure loss of the $11\frac{1}{2}^{\circ}$ diffuser with cast straightening vanes was 0.027 compared with 0.035 for the sheet-metal straightening vanes. In view of the more effective reduction in tail-pipe pressure loss and the more uniform diffuser-outlet velocity profile obtained with the cast straightening vanes, these straightening vanes were used for the remainder of the investigation.

Effect of diffusion rate. - Diffuser configurations with three different diffusion rates, all employing the cast straightening vanes, were investigated to determine the effect of diffusion rate on over-all diffuser performance. The variation of diffuser area with length ratio for the three diffusers investigated is shown in figure 8; also shown is the

area variation of an 18-inch conical innerbody diffuser, which had the lowest pressure loss of the diffusers investigated in reference 1. It should be noted in figure 8 that each of the diffusers investigated had a different area expansion ratio up to the end of the innerbody; therefore, the diffusers had varying amounts of sudden expansion losses. However, the maximum variation in projected area at the end of the innerbody, for the innerbodies investigated, is only 7.5 percent of the final diffuser area.

The bar graph in figure 9 illustrates the tail-pipe pressure loss obtained with the $11\frac{1}{2}^{\circ}$, 15°, and 20° diffusers and also with the 18-inch conical innerbody diffuser of reference 1. The $11\frac{1}{2}^{\circ}$ diffuser, which had a tail-pipe pressure-loss ratio of 0.027, had the lowest pressure loss and the lowest diffusion rate of the configurations investigated. The increase in pressure loss of the 15° diffuser over that of the $11\frac{1}{2}^{\circ}$ diffuser was only 0.007, compared with an increase of 0.049 for the 20° diffuser over that of the 15° diffuser. The pressure loss of the $11\frac{1}{2}^{\circ}$ diffuser was less than one-half the pressure loss of the 18-inch conical innerbody diffuser of reference 1. Part of this improvement is attributed to improved straightening vanes and the remainder to the decrease in overall diffusion rate before the end of the innerbody.

The diffuser-outlet velocity profiles for the $11\frac{1}{2}^{\circ}$, 15°, and 20° diffusers are shown in figure 10. The 20° diffuser has a severe velocity gradient with velocities over 1000 feet per second existing near the outer wall. Even though the pressure measurements used to obtain the velocity profile were made 4 inches downstream of the innerbody of the 20° diffuser (see sketch in fig. 10), the flow appears to be separated before the end of the innerbody. This flow separation from the innerbody accounts for the large increase in pressure loss of the 20° diffuser over that of the 15° diffuser.

Afterburner Pressure Losses

The pressure losses of the afterburning components (spray bars, flameholder, and liner) are presented in figure 11. The component pressure loss was defined as the ratio of the increase in loss of total pressure between turbine discharge and exhaust-nozzle inlet to turbine-discharge total pressure, resulting from the addition of each individual component. Fuel systems with both 28 and 16 spray bars were used for afterburning. The pressure loss of 28 round spray bars, located 5.25 inches downstream of the diffuser inlet, was 0.013. Because local flow Mach numbers in excess of 0.5 existed in the region of fuel injection, the 28 spray bars were flattened or faired (fig. 5) in an attempt to

reduce the pressure loss. As a result of fairing the 28 spray bars, the pressure loss was reduced from 0.013 to 0.003. The pressure loss of 16 faired spray bars was approximately 0.001. Flameholder and acoustic-liner pressure losses were 0.019 and 0.006, respectively. Except for the diffuser, the flameholder pressure loss was the highest of the afterburner component pressure losses.

The over-all pressure loss of short-afterburner configurations composed of the $11\frac{1}{2}^{15}$ diffuser with 59 cast straightening vanes, 28 faired spray bars, a flameholder, and a liner was 5.5 percent of the turbine-discharge total pressure, which is about 3 percentage points lower than the short afterburner of reference 2. The pressure loss of the standard-engine tail pipe (fig. 3(c)) was found to be 5.6 percent of the turbine-discharge total pressure; thus the pressure loss of the short afterburner is about equal to that of the standard engine tail pipe.

3678

Afterburner Performance

Afterburning. - Two short-afterburner configurations, which differed only in fuel systems, were investigated. The first fuel system consisted of 28 round spray bars injecting fuel upstream, and the second fuel system had 16 spray bars injecting fuel normal to the flow. Afterburner performance data were not obtained with a fuel system composed of 28 faired spray bars. However, it was felt that the combustion efficiency would not be appreciably different from that obtained with the 28 round spray bars. Both afterburners used the $11\frac{1}{2}^{10}$ diffuser with the cast straightening vanes. Afterburner combustion performance data were obtained with three fixed-area conical nozzles. As a result, three over-all fuel-air ratios were obtainable at an engine speed of 7800 rpm and a turbine-discharge temperature of 1240° F.

Over-all afterburner performance is presented in figure 12 for both configurations. In figure 12(a) afterburner-outlet temperature is shown as a function of over-all fuel-air ratio with lines of constant combustion efficiency superimposed. Afterburner-outlet temperature was calculated from the measured thrust, mass flow, and exhaust-nozzle pressure ratio. Afterburner combustion efficiency was defined as the ratio of actual afterburner temperature rise to ideal temperature rise. The ideal temperature rise was obtained from reference 6. A peak combustion efficiency of 0.95 was obtained for the 28-spray-bar configuration at a fuel-air ratio of 0.045, as compared with 0.83 for the 16-spray-bar configuration at a fuel-air ratio of 0.042. The superior performance of the 28-spray-bar configuration at higher fuel-air-ratio levels was a result of a more uniform circumferential fuel distribution. This characteristic is also illustrated in reference 7. The combustion efficiency of both afterburner configurations decreased 15 to 20 percentage points for an increase in over-all fuel-air ratio from 0.045 to 0.070. This severe decrease in combustion efficiency approaching the stoichiometric fuel-air

ratio is partially a result of the lean region near the outer shell provided for cooling the afterburner shell and liner. At high fuel-air ratios this lean region causes the local fuel-air ratio in the remainder of the flow passage to be richer than stoichiometric, consequently reducing combustion efficiency. Afterburner performance for configuration 4 of reference 2 is also included for comparison in figure 12(a).

The variation of augmented thrust ratio with over-all fuel-air ratio for the two afterburner configurations is shown in figure 12(b). This figure also includes an ideal augmented-thrust-ratio curve, which considers the momentum pressure loss during heat addition based on a bulk velocity of approximately 400 feet per second. A peak thrust augmentation ratio of 1.44 was obtained with the 28-spray-bar configuration at an over-all fuel-air ratio of 0.061. Increasing the over-all fuel-air ratio above 0.061 for both configurations resulted in a decrease in augmented thrust ratio as a result of the severe drop in combustion efficiency. As a result of the higher combustion efficiencies of the 28-spray-bar configuration as compared with the 16-spray-bar configuration, the augmented thrust ratios were 2 to 5 percentage points higher. Differences between the ideal and actual augmented-thrust-ratio curves resulted from combustion inefficiency and higher-than-estimated momentum pressure loss. The actual momentum pressure loss averaged 4 percentage points higher than calculations based on an afterburner-inlet bulk velocity. The augmented thrust ratio of a short afterburner with a fuel system composed of 28 faired spray bars would be approximately 1 percent higher than for the short afterburner with 28 round spray bars because the tail-pipe pressure loss is 1 percent lower.

Throughout the afterburning portion of the investigation, no serious outer-shell hot spots or evidence of combustion screech was encountered. The absence of afterburner hot spots and screech is attributed to the perforated liner. No liner damage was noted during the investigation.

Nonafterburning. - For application of the short afterburner to long-range aircraft, the nonafterburning performance of the short afterburner is important from considerations of engine fuel economy during cruise flight conditions. Although engine cruise conditions were not simulated during the investigation, the nonafterburning performance obtained is a close approximation of the cruise performance. Since the thrust of the engine is approximately proportional to the exhaust-nozzle total pressure, tail-pipe pressure losses result in a reduction in thrust and consequently an increase in specific fuel consumption. Because the nonafterburning tail-pipe pressure loss of the short afterburner with 28 faired spray bars was approximately equal to that of the standard nonafterburning engine, the specific fuel consumption of the engine equipped with a short afterburner would be approximately equal to that of the standard engine.

SUMMARY OF RESULTS

The following results were obtained from an investigation of the problems associated with the design of a low-pressure-loss, short afterburner for sea-level thrust augmentation.

It was found that turbine-discharge whirl resulted in sizable diffuser pressure losses. These losses were reduced by the addition of flow-straightening vanes at the turbine discharge. An afterburner diffuser consisting of a cylindrical outer shell and a $11\frac{1}{2}^{\circ}$, blunt-end innerbody had a lower pressure loss than either a 15° or 20°, blunt-end innerbody diffuser. The increase in tail-pipe pressure loss due to the afterburner spray bars was important in short-afterburner installations where fuel spray bars are located in high Mach number, turbine-discharge flow. The pressure loss of 28 round spray bars was reduced from 0.013 to 0.003 by fairing (flattening) these spray bars. The tail-pipe pressure loss of one of the short-afterburner configurations was 0.055, which was approximately equal to that of the standard-engine tail pipe.

The peak afterburner combustion efficiency increased 12 percentage points by changing from a 16- to a 28-spray-bar fuel system. A peak combustion efficiency of 0.95 was obtained at a fuel-air ratio of 0.042 for the short afterburner with the 28-spray-bar fuel system. A maximum augmented thrust ratio of 1.44 was obtained for the short-afterburner configuration with 28 spray bars at a fuel-air ratio of 0.061. The specific fuel consumption of the engine equipped with a short afterburner while operating at cruise conditions was expected to be equal to that of the standard nonafterburning engine because the tail-pipe pressure losses were approximately equal.

Lewis Flight Propulsion Laboratory
National Advisory Committee for Aeronautics
Cleveland, Ohio, April 26, 1955

REFERENCES

1. Mallett, William E., and Harp, James L., Jr.: Performance Characteristics of Several Short Annular Diffusers for Turbojet Engine Afterburners. NACA RM E54B09, 1954.

2. Harp, James L., Jr., Mallett, William E., and Shillito, Thomas B.: Experimental Sea-Level Static Investigation of a Short Afterburner. NACA RM E54B18, 1954.

3. Wood, Charles C., and Higginbotham, James T.: The Influence of Vortex Generators on the Performance of a Short 1.9:1 Straight-Wall Annular Diffuser with a Whirling Inlet Flow. NACA RM L52L01a, 1953.

4. Wood, Charles C., and Higginbotham, James T.: Flow Diffusion in a Constant-Diameter Duct Downstream of an Abruptly Terminated Center Body. NACA RM L53D23, 1953.

5. Wood, Charles C., and Higginbotham, James T.: Performance Characteristics of a 24° Straight-Outer-Wall Annular-Diffuser-Tailpipe Combination Utilizing Rectangular Vortex Generators for Flow Control. NACA RM L53H17a, 1953.

6. Mulready, Richard C.: The Ideal Temperature Rise Due to the Constant Pressure Combustion of Hydrocarbon Fuels. M.I.T. Meteor Rep. UAC-9, Res. Dept., United Aircraft Corp., July 1947. (BuOrd Contract NOrd 9845.)

7. Jansen, Emmert T., Velie, Wallace W., and Wilsted, H. Dean: Experimental Investigation of the Effect of Fuel-Injection-System Design Variables on Afterburner Performance. NACA RM E53K16, 1954.

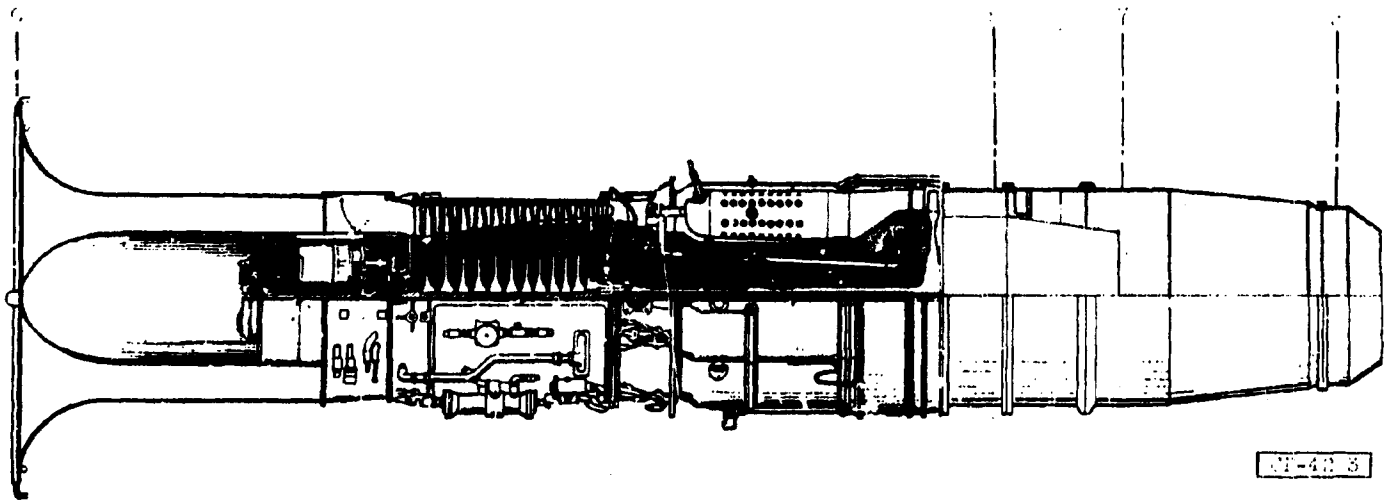

Station	Location	Thermocouples		Total pressure	
		Rakes	Probes	Rakes	Probes
0	Engine inlet	2	20	-	-
5	Turbine outlet	6	24	4	16
7[a]	Diffuser outlet	-	-	3	12
9	Exhaust-nozzle inlet	1	14	1	16

[a]Wedge probe was installed here for diffuser tests.

Figure 1. - Cross section of engine showing instrumentation stations.

3678

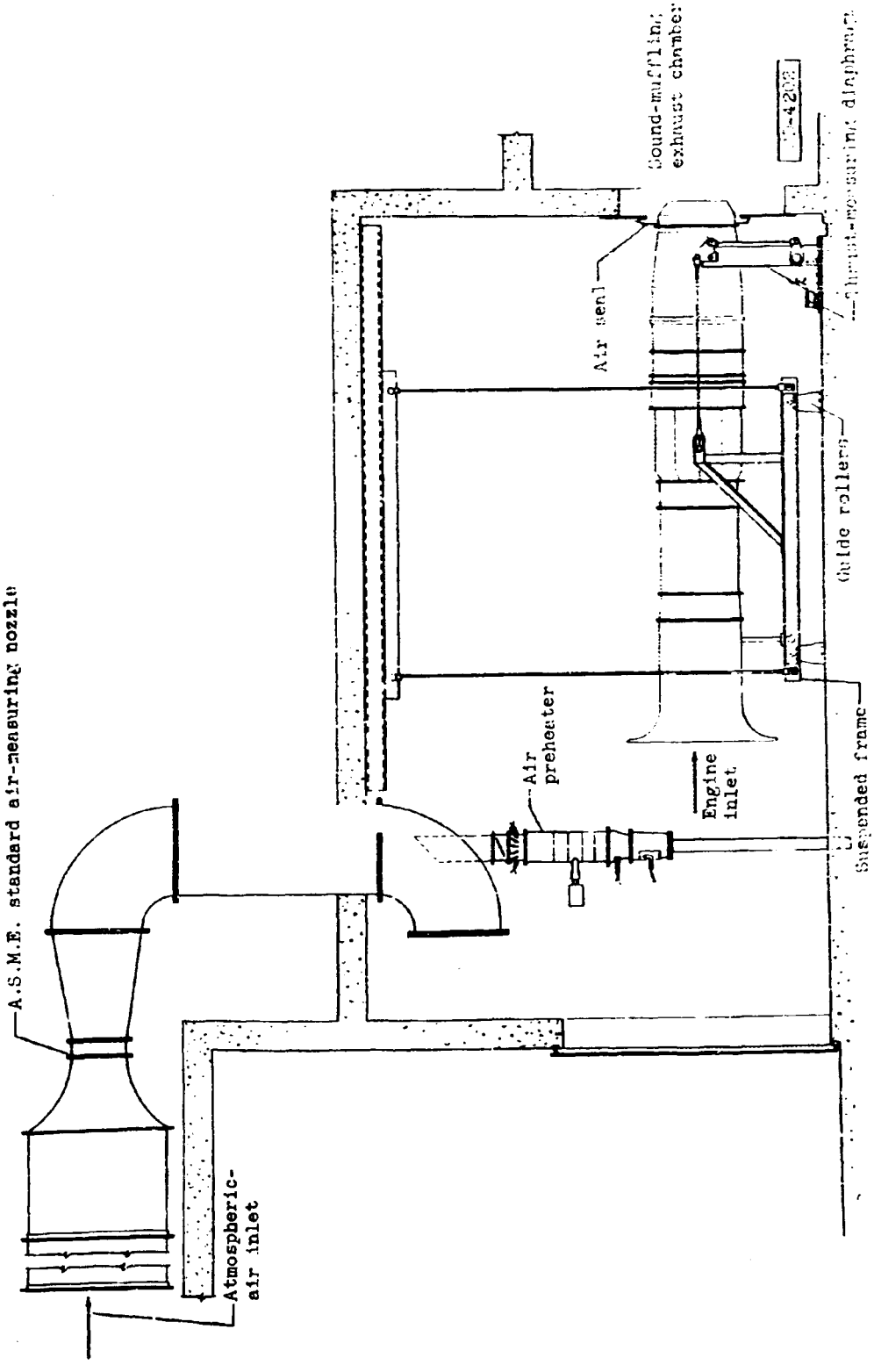

Figure 2. - Schematic diagram of installation of engine in test cell.

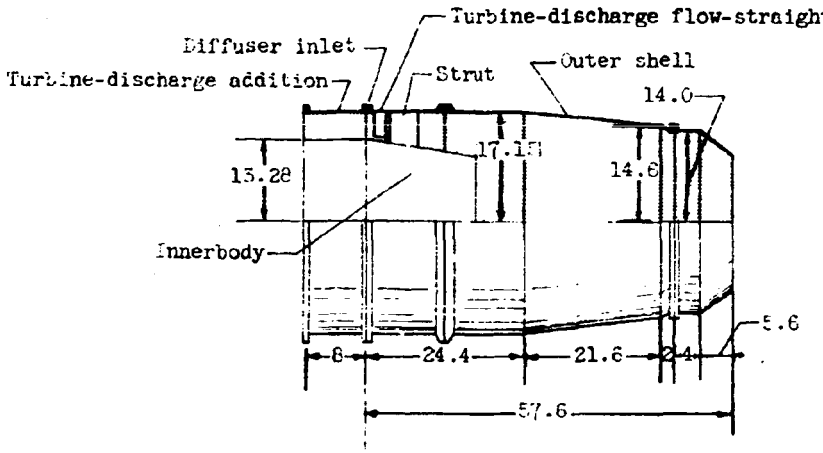

(a) Typical afterburner outer shell and innerbody assembly for diffuser tests.

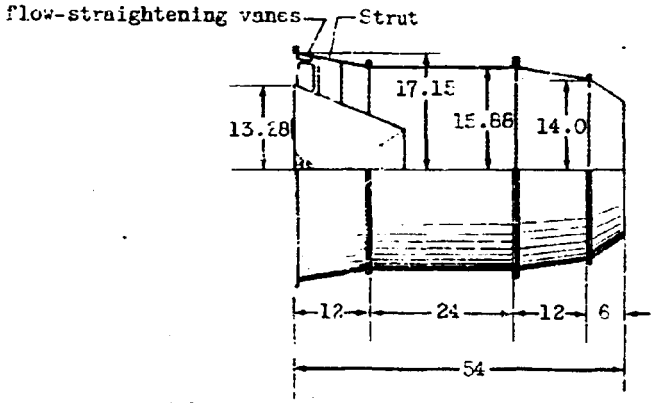

(b) 16-Inch conical innerbody diffuser (ref.1).

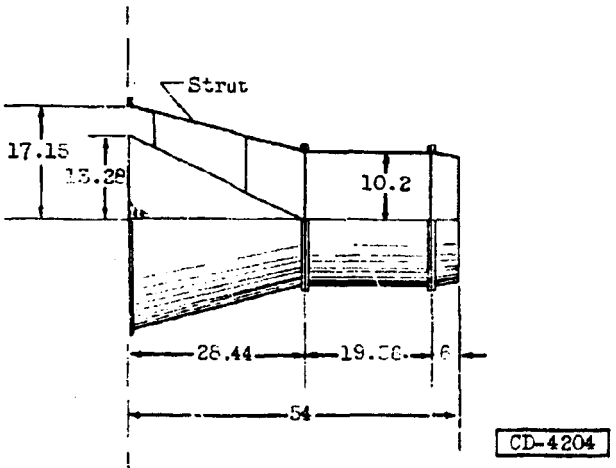

(c) Standard tail pipe.

Figure 3. - Short afterburner and standard engine tail pipes. (All dimensions in inches.)

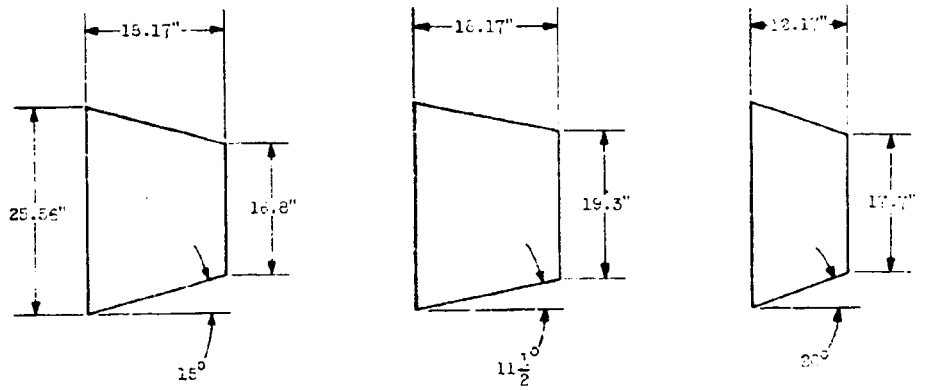

(a) Innerbodies.

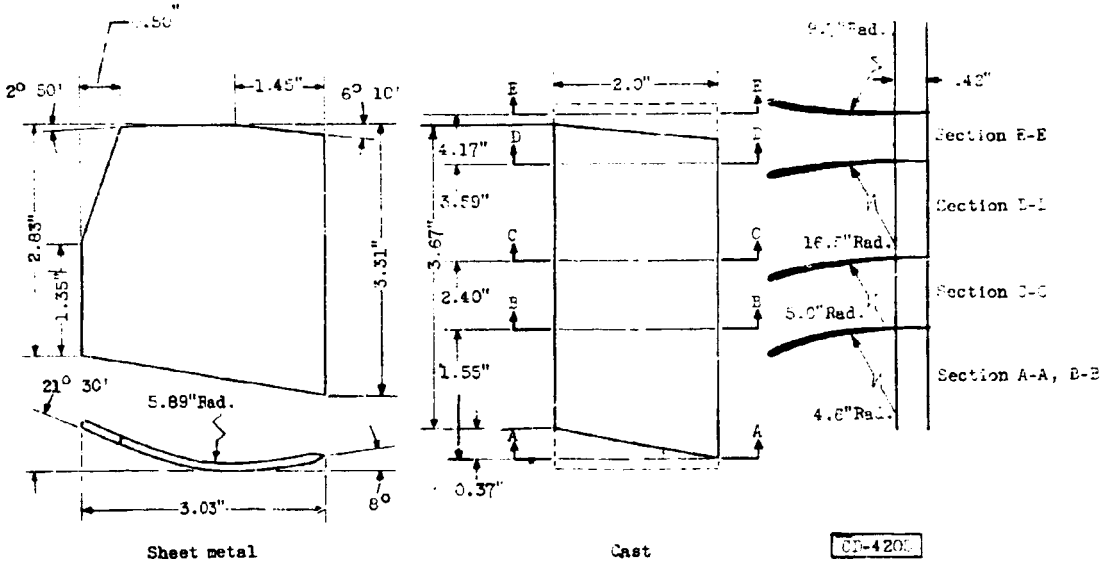

(b) Flow-straightening vane.

Figure 4. - Innerbodies and turbine-discharge flow-straightening vanes.

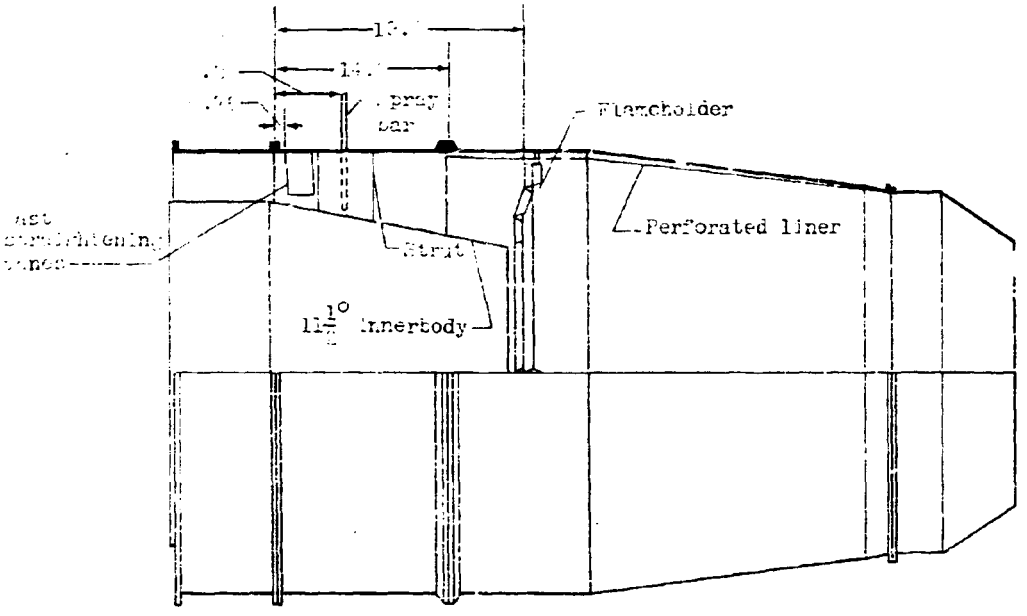

(a) Afterburner assembly details.

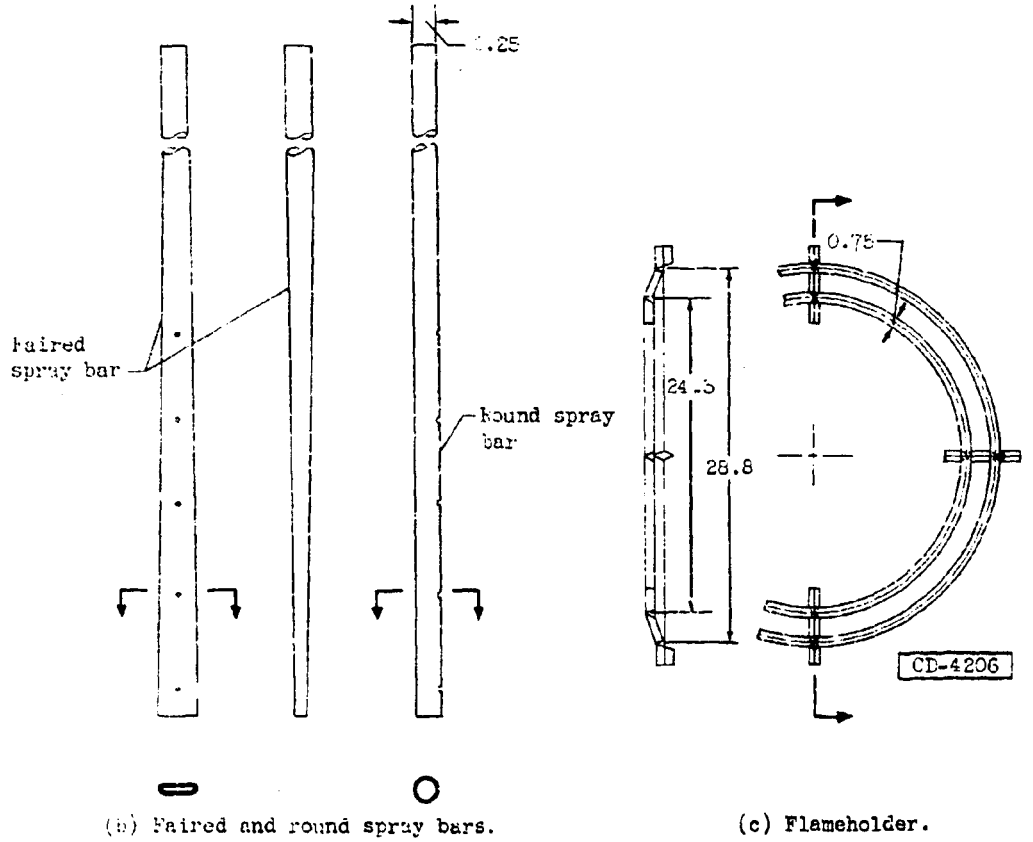

(b) Faired and round spray bars.

(c) Flameholder.

Figure 5. - Typical short-afterburner assembly. (All dimensions in inches.)

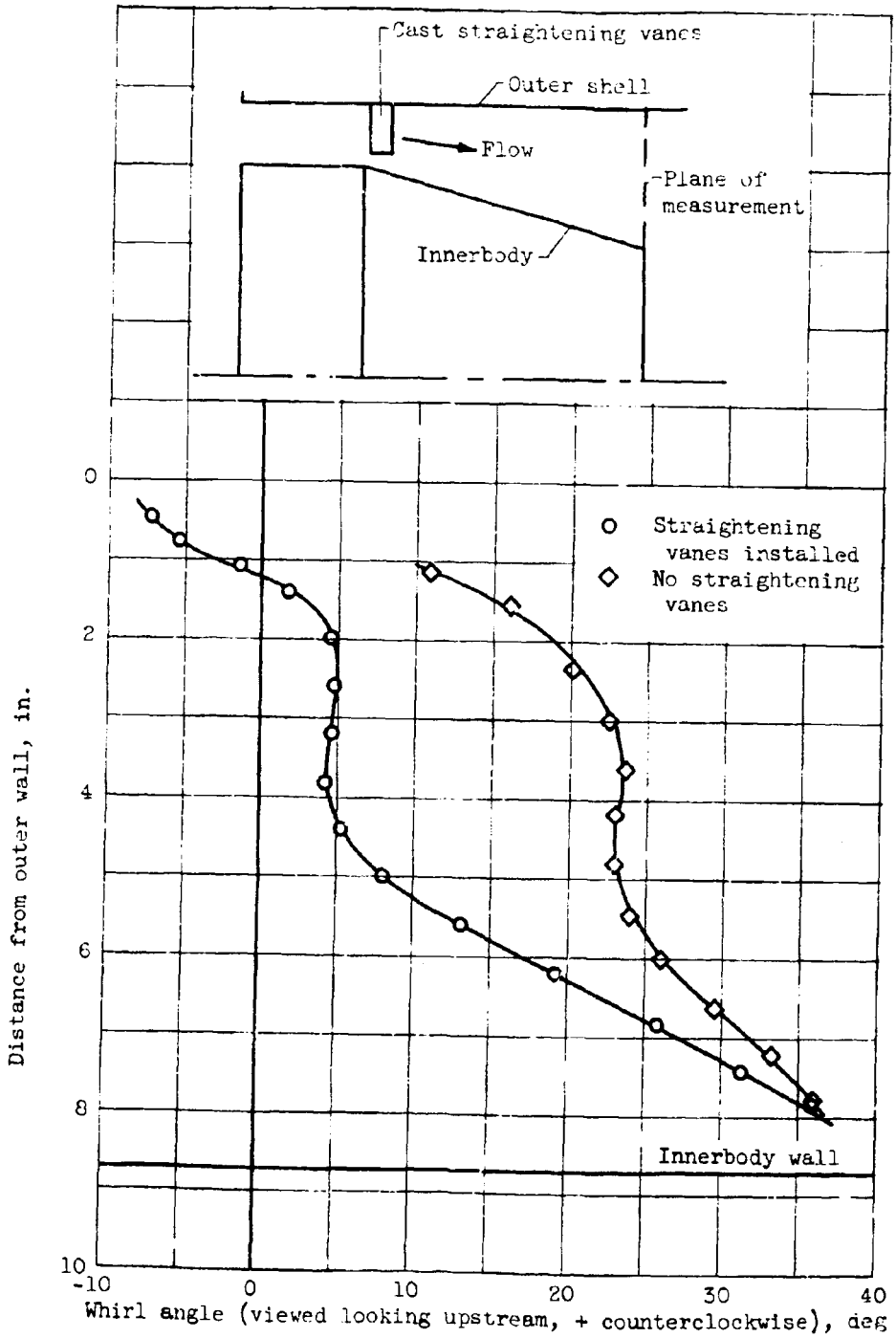

(a) Whirl profiles at diffuser outlet.

Figure 6. - Effect of cast straightening vanes on diffuser-outlet whirl and velocity profiles for 15° diffuser.

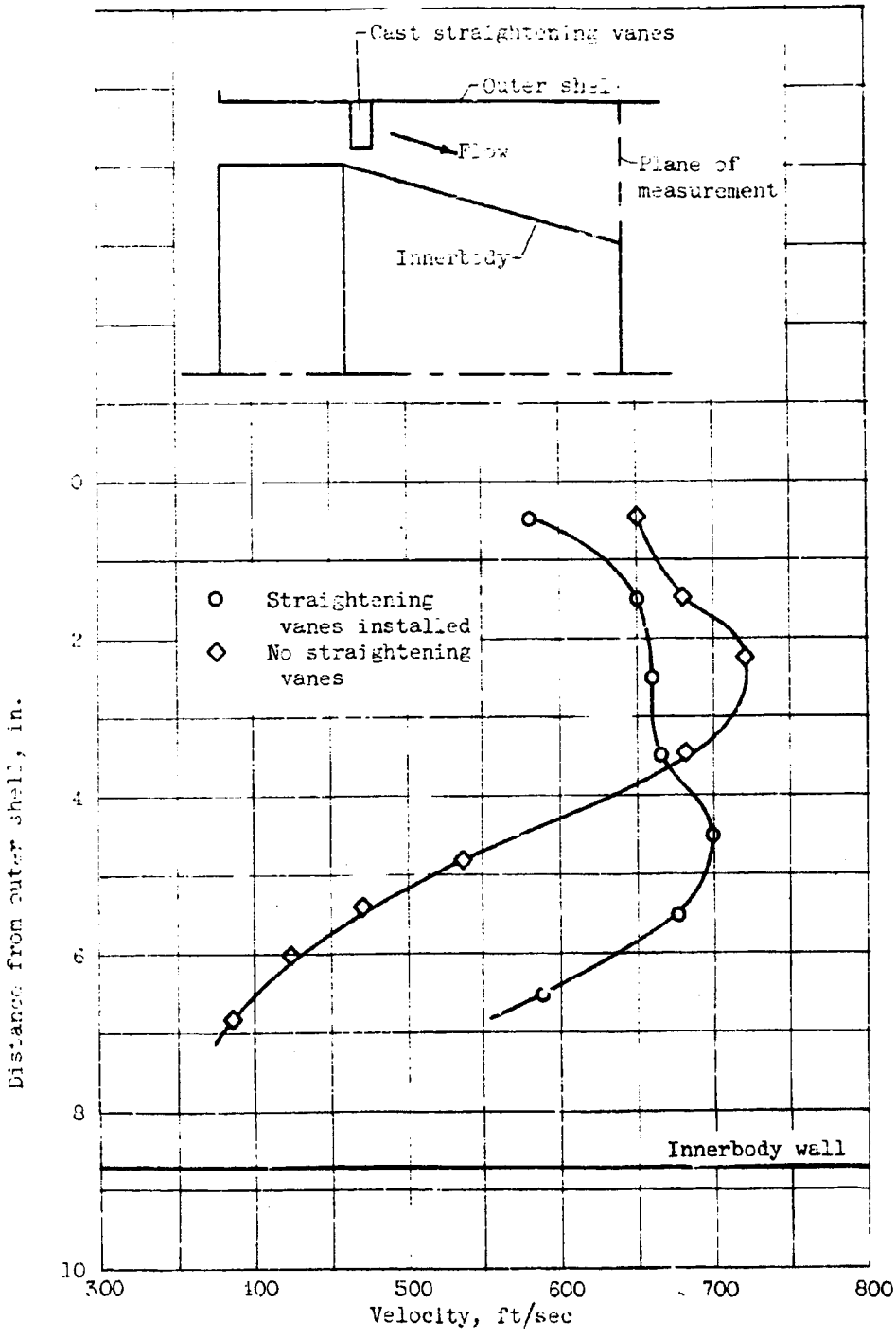

(b) Velocity profiles at diffuser outlet.

Figure 6. - Concluded. Effect of cast straightening vanes on diffuser-outlet whirl and velocity profiles for 15° diffuser.

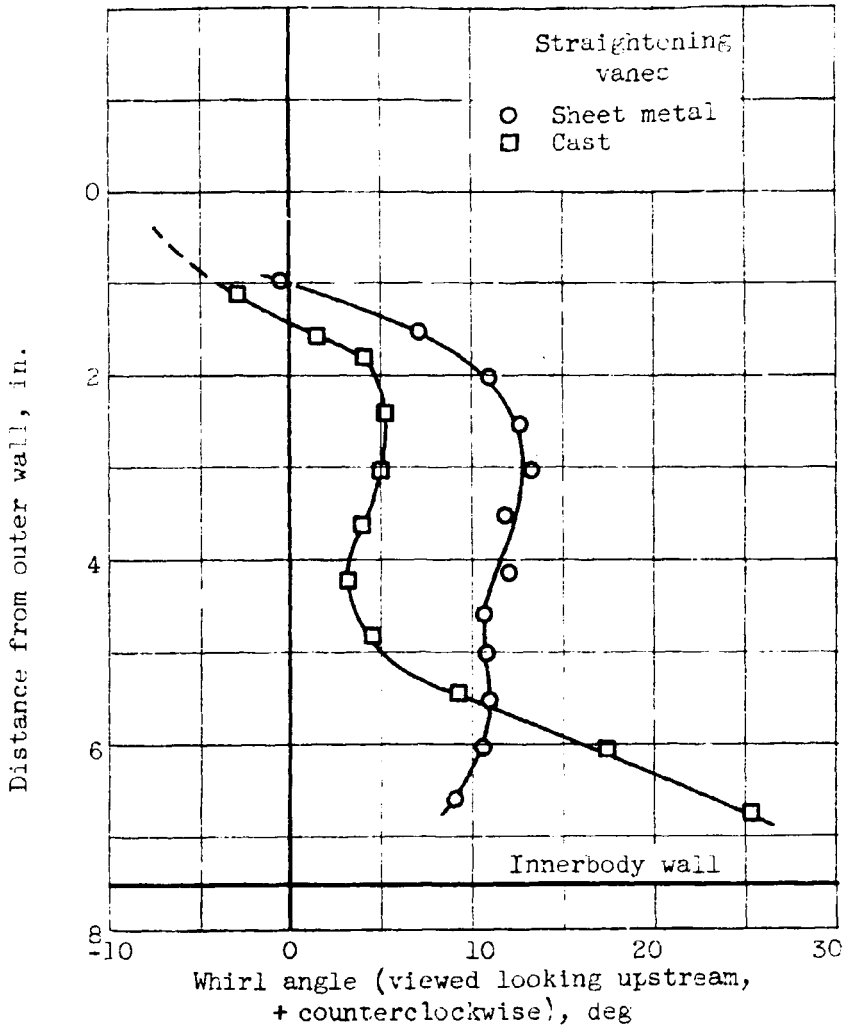

(a) Whirl profile.

Figure 7. - Comparison of diffuser-outlet whirl and velocity profiles of $11\frac{10}{2}$ diffuser with either sheet-metal or cast straightening vanes installed.

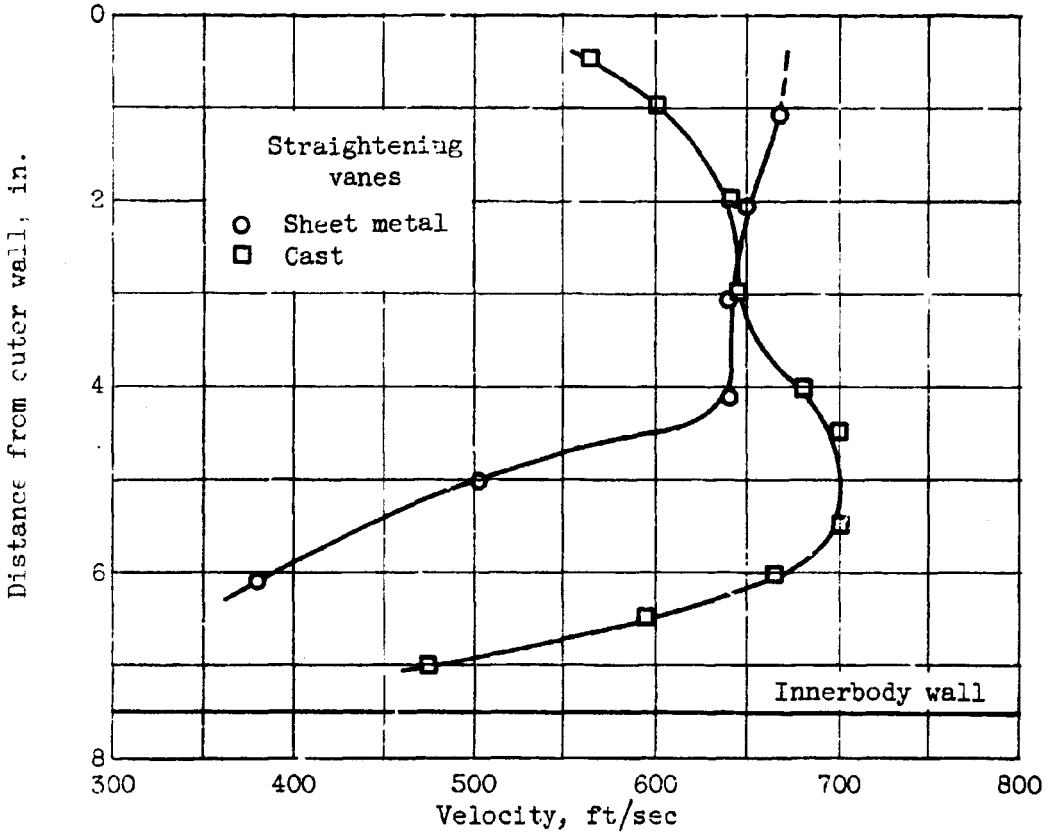

(b) Velocity profiles.

Figure 7. - Concluded. Comparison of diffuser-outlet whirl and velocity profiles of $11\frac{1}{2}^{\circ}$ diffuser with either sheet-metal or cast straightening vanes installed.

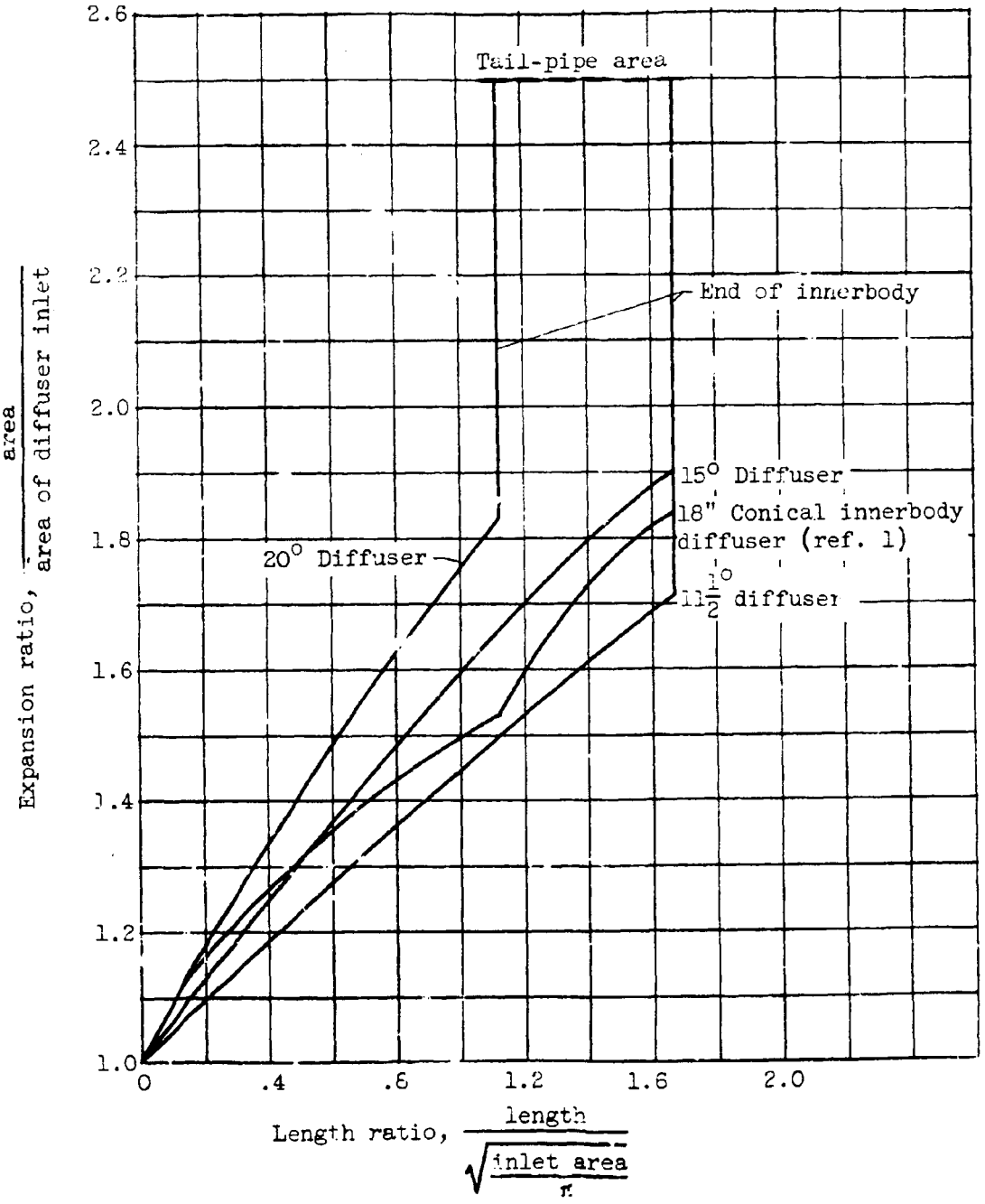

Figure 8. - Variation of diffuser area with length ratio.

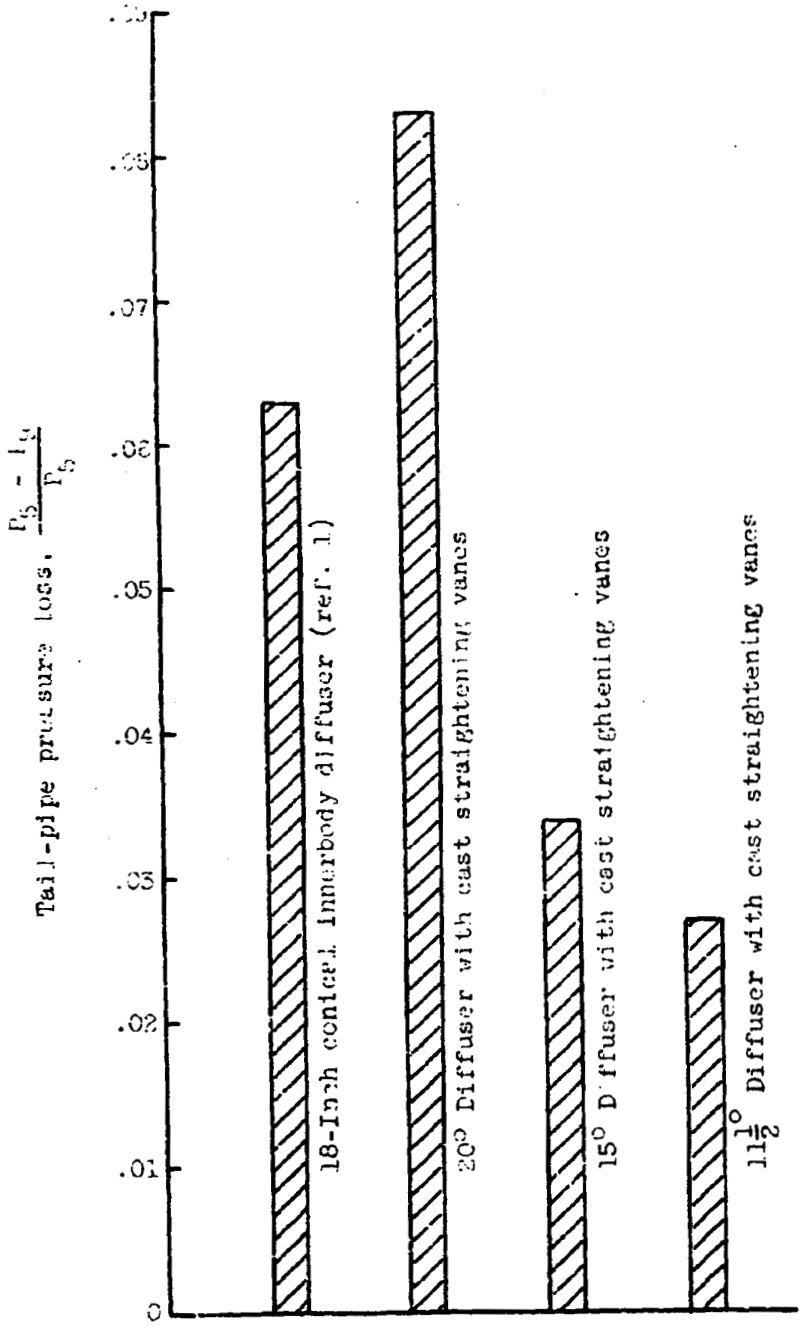

Figure 9. - Comparison of tail-pipe pressure losses of four diffusers.

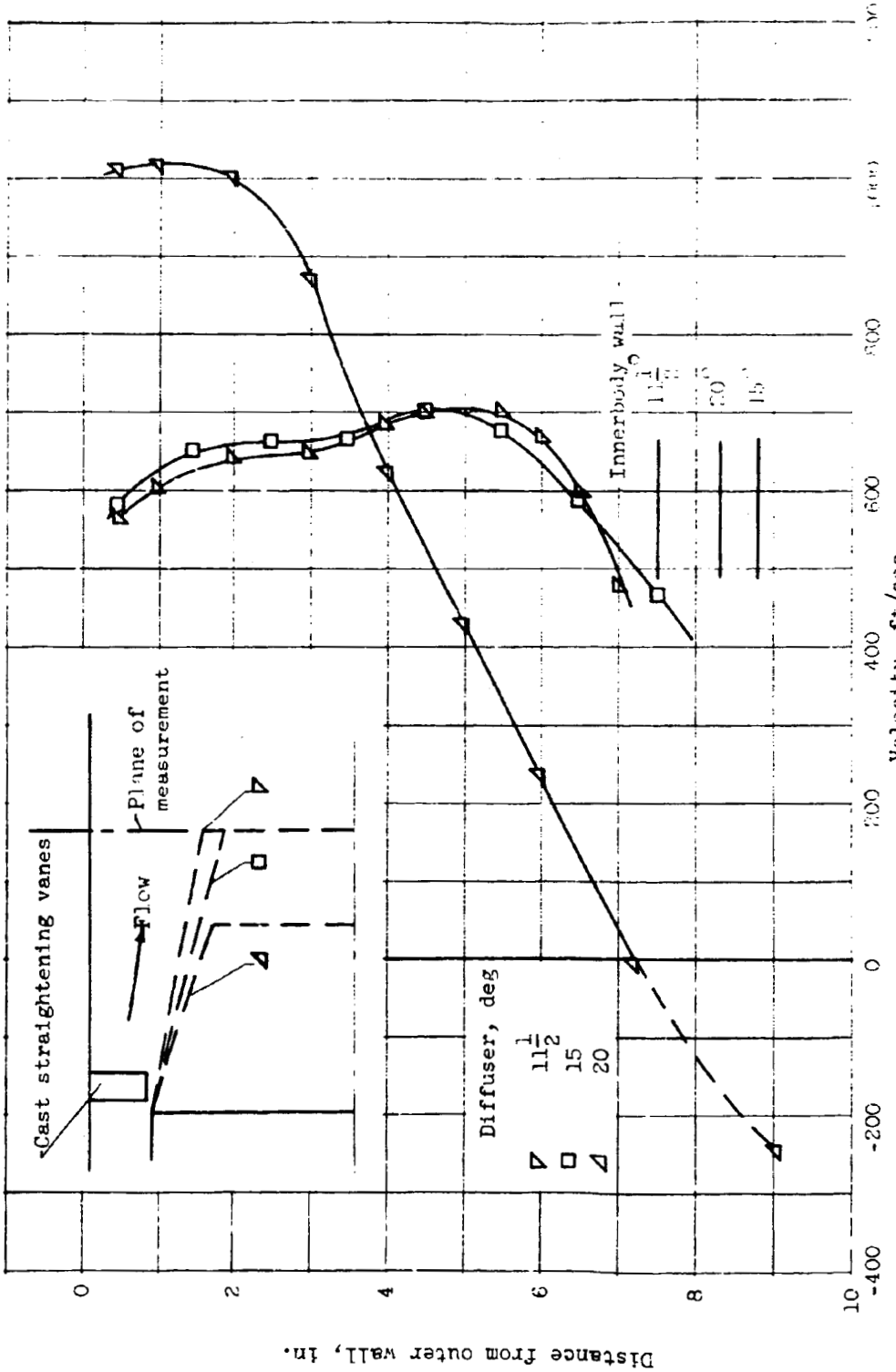

Figure 10. - Comparison of velocity profiles of three diffusers with cast straightening vanes installed.

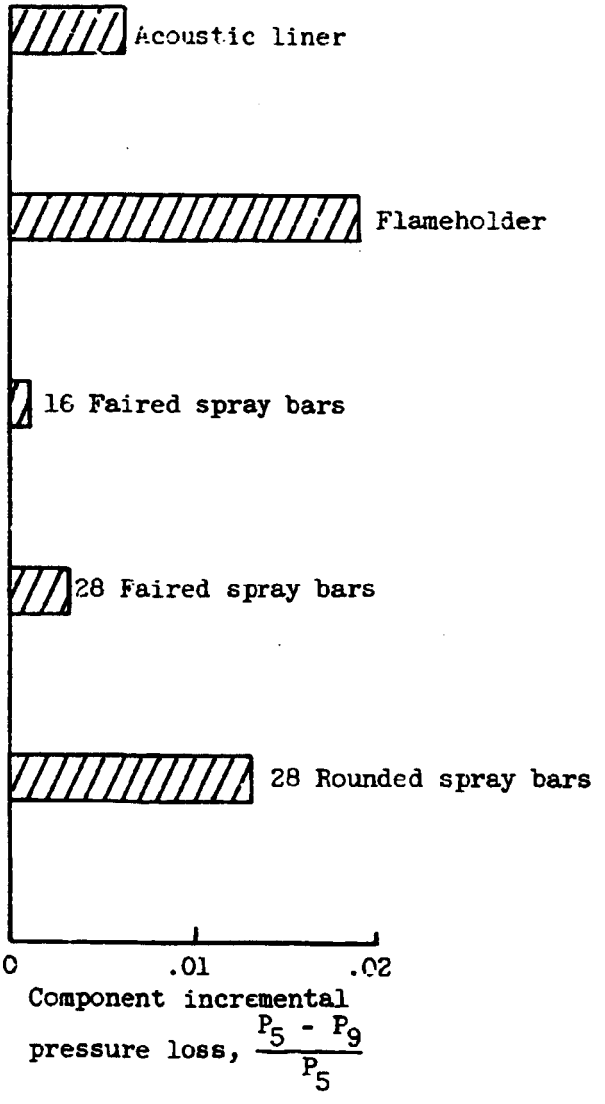

Figure 11. - Afterburner-component pressure losses.

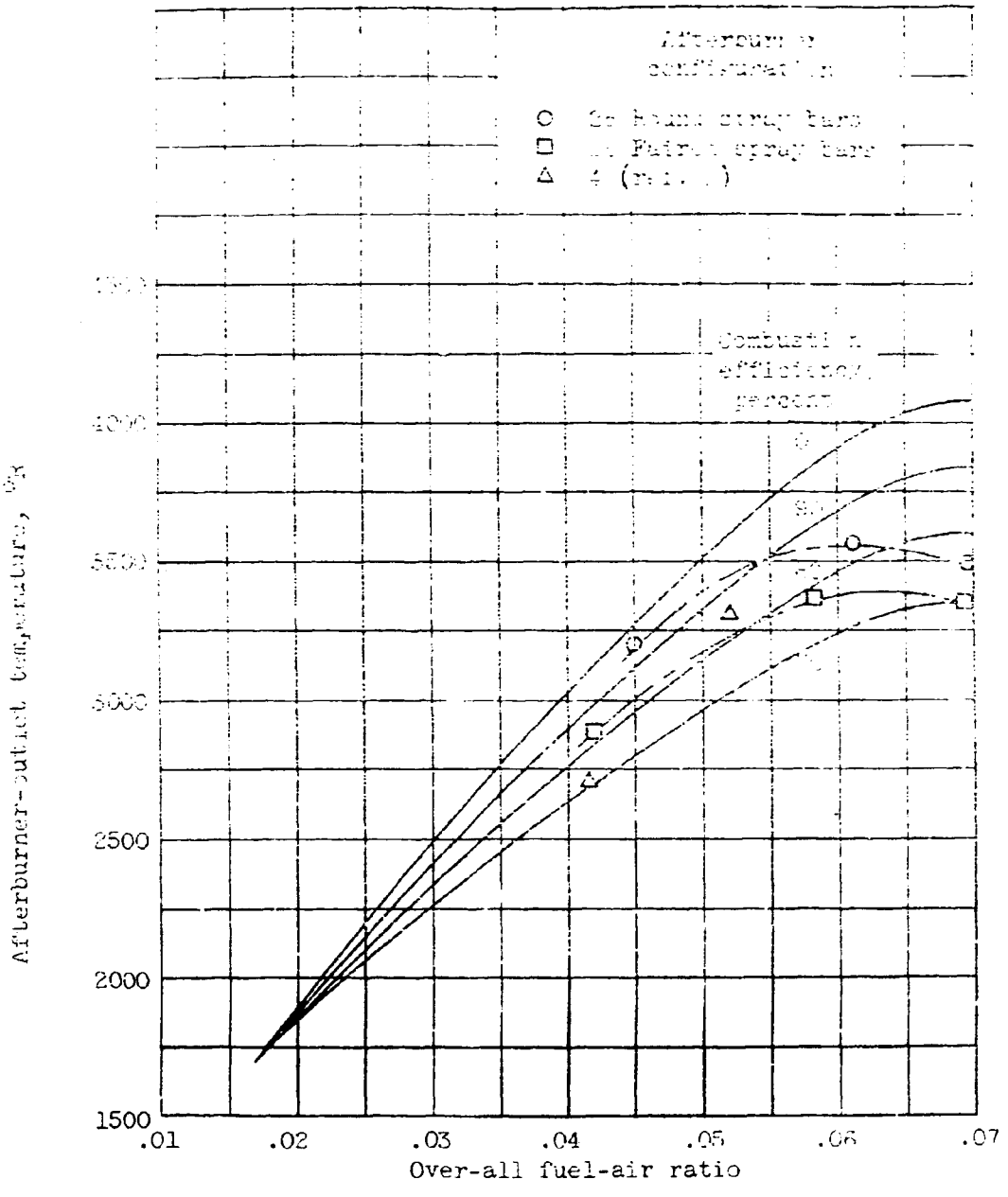

(a) Afterburner-outlet temperature and combustion efficiency.

Figure 12. - Afterburner performance.

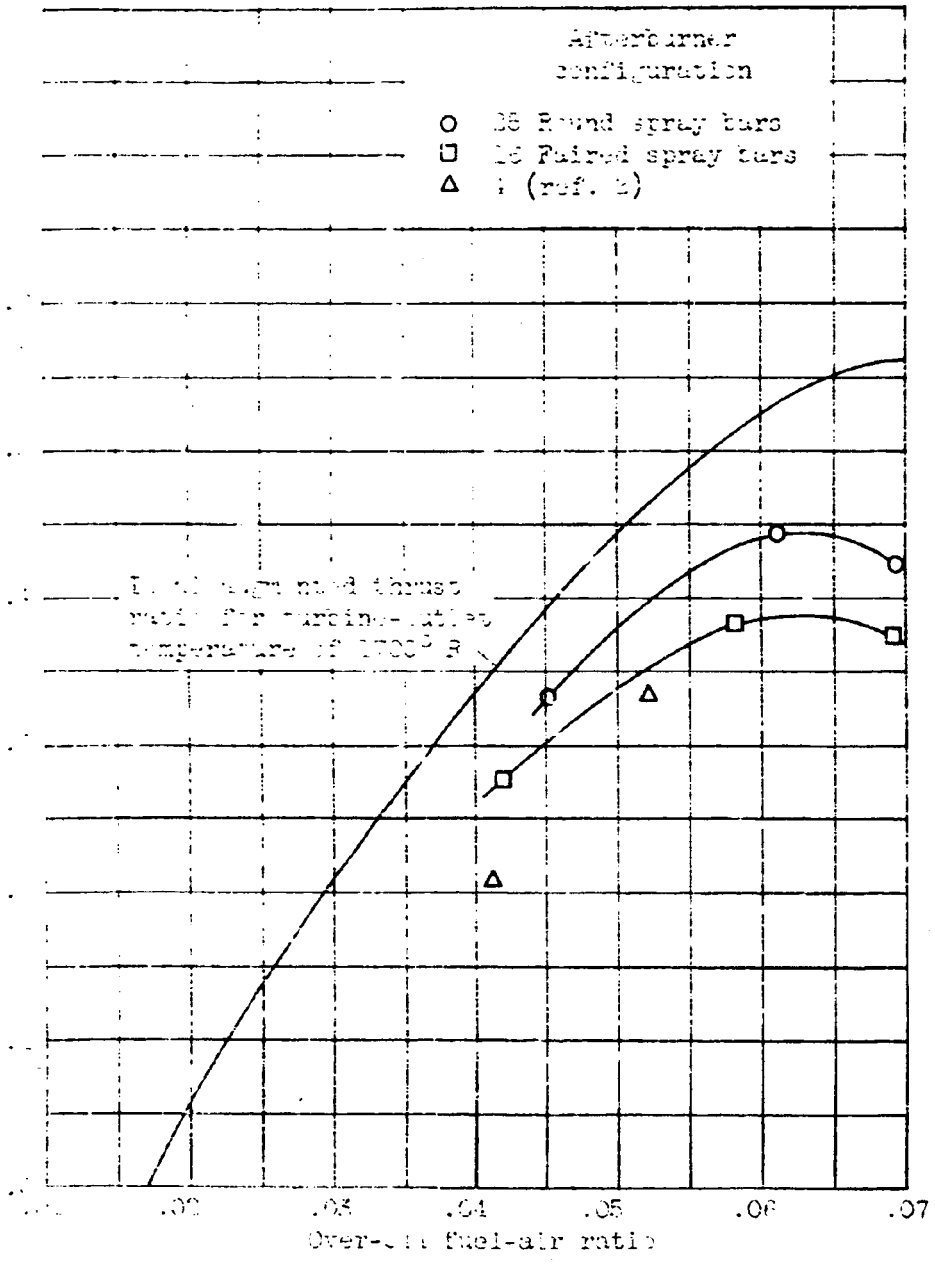

(b) Augmented thrust ratios.

Figure 11. - Concluded. Afterburner performance.